

Impact of Preprocessing on Neural Network-Based RSS/AoA Positioning

Omid Abbassi Aghda^{1,2}, Slavisa Tomic^{3,4}, Oussama Ben Haj Belkacem^{1,5}, João Guerreiro^{1,2}, Nuno Souto^{1,6}, Michal Szczachor^{2,7}, and Rui Dinis^{1,2}

¹Instituto de Telecomunicações, Lisboa, Portugal

²Universidade Nova de Lisboa, Monte da Caparica, 2829-516 Caparica, Portugal

³UNINOVA-CTS – Center of Technology and Systems, NOVA School of Science and Technology, 2829-516 Caparica, Portugal

⁴COPELABS, ECATI, Lusófona University, 1749-024 Lisbon, Portugal

⁵Innov'Com Laboratory, Sup'Com, University of Carthage, Tunis 1054, Tunisia

⁶ISCTE-Instituto Universitário de Lisboa, 1649-026 Lisbon, Portugal

⁷Nokia, Wroclaw, Poland

Abstract—Hybrid received signal strength (RSS)/angle of arrival (AoA)-based positioning offers low-cost distance estimation and high-resolution angular measurements. Still, it comes at a cost of inherent nonlinearities, geometry-dependent noise, and suboptimal weighting in conventional linear estimators that might limit accuracy. In this paper, we propose a neural network-based approach using a multilayer perceptron (MLP) to directly map RSS/AoA measurements to 3D positions, capturing nonlinear relationships that are difficult to model with traditional methods. We evaluate the impact of input representation by comparing networks trained on raw measurements versus preprocessed features derived from a linearization method. Simulation results show that the learning-based approach consistently outperforms existing linear methods under RSS noise across all noise levels, and matches or surpasses state-of-the-art performance under increasing AoA noise. Furthermore, preprocessing measurements using the linearization method provides a clear advantage over raw data, demonstrating the benefit of geometry-aware feature extraction.

Index Terms—Deep learning, 3D localization, received signal strength (RSS), angle of arrival (AoA), weighted least squares (WLS)

I. INTRODUCTION

Fifth-generation wireless system (5G) wireless systems are designed to support a diverse set of use cases, including enhanced mobile broadband (eMBB), ultra-reliable low-latency communications (URLLC), and massive machine-type communications (mMTC). Beyond data transmission, these use cases increasingly rely on accurate situational awareness to enable higher-layer applications such as Internet of Things (IoT) services, vehicle-to-everything communication (V2X) communication, unmanned aerial vehicle (UAV)s, and autonomous vehicular systems. In such applications, awareness of the position of communicating devices or targets, such as vehicles

This work was conducted within the MiFuture project, which has received funding from the European Union's Horizon Europe (HE) Marie

Skłodowska-Curie Actions MiFuture HORIZON-MSCA2022-DN-01, under Grant Agreement number 101119643 and YAHYA/6G HORIZON-MSCA-2022-PF-01, under Grant Agreement number 101109435. It was partially supported by FCT/MECI through national funds and when applicable co-funded EU funds under UID/50008: Instituto de Telecomunicações.

or drones, is essential for safe and efficient operation. Consequently, wireless positioning has emerged as a key enabling technology that must be addressed alongside communication performance. Looking ahead, it is widely anticipated that in sixth-generation wireless system (6G) systems, positioning and communication will be even more tightly integrated, with location information actively supporting communication, sensing, and control functions [1], [2].

One common approach for positioning is to use received signal strength (RSS) and angle of arrival (AoA) measurements collected from sensors. RSS information is attractive due to its low cost, while angular measurements can be obtained efficiently in multi-antenna multiple-input multiple-output (MIMO) systems. A well-studied research direction is to transform the inherently nonlinear positioning problem based on RSS and AoA into a linear form to enable closed-form solutions. For example, in [3], the authors approximate the nonlinear model using a Taylor series expansion and a Cartesian-to-spherical transformation, resulting in a linearized system that can be solved via weighted least squares (WLS). Similarly, the approach in [4] applies an alternative linearization method and uses a standard least square (LS) estimator to solve the resulting system. Subsequent work in [5] extends this approach by adding constraints to the WLS cost function, reformulating it as a generalized trust region subproblem (GTRS), and solving it efficiently using a bisection procedure. Despite their computational efficiency, these methods remain limited in practice. RSS- and AoA-based positioning suffers from model nonlinearities, multipath propagation, and noise interference, which reduce accuracy in real-world deployments. Moreover, linearization based on Taylor approximations introduces errors, and the resulting WLS solution is generally suboptimal under realistic noise conditions [6], [7]. In addition, the weighting matrices used in WLS are typically heuristic or approximate, and non-optimal weighting can further degrade performance, especially when measurement noise is heterogeneous across anchors [7].

The use of aritifical intelegence (AI) techniques is

widespread in positioning problems. In particular, deep learning (DL)-based models are well suited for capturing nonlinear relationships and can effectively model the nonlinearities inherent in hybrid RSS/AoA positioning [8]. Moreover, the positioning problem is inherently geometry-dependent, and preprocessing has a significant impact on the performance of DL-based systems [9]. Therefore, the system structure and input representation should be explicitly considered rather than relying solely on raw measurements. Consequently, analyzing whether to use preprocessed geometric features or raw measurements is essential to determine which approach enables more effective learning.

In this paper, we propose a neural network-based approach to address the nonlinearities inherent in hybrid RSS/AoA positioning, as studied in [3], [5]. Specifically, we design and train a multilayer perceptron (MLP) network to learn the mapping from measurements to 3D positions, capturing nonlinear relationships that are difficult to model with conventional linear estimators. In addition, we evaluate the impact of input representation by comparing networks trained on raw measurements versus preprocessed features derived from the linearization method in [3], allowing us to quantify how geometry-aware preprocessing can enhance learning performance.

Although WLS approach provides a computationally efficient estimator, its performance is limited in practice due to linearization errors, noise propagation, and potentially sub-optimal weighting. By leveraging MLP, our approach can implicitly compensate for these limitations, learning a mapping that mitigates nonlinearities, weighting biases, and geometry-dependent errors, resulting in more robust positioning. To validate our method, we plot the root mean square error (RMSE) versus noise variance for both RSS and AoA measurements. The results show that the MLP-based approach consistently outperforms the methods in [3]–[5] in the presence of RSS noise across all noise levels. For increasing AoA noise, the proposed method yields lower RMSE than [4], [5], while achieving RMSE performance comparable to [3]. Furthermore, using the same network architecture, preprocessing the measurements via the linearization method provides a clear advantage over training with raw data, demonstrating the benefit of geometry-aware feature extraction.

II. PROBLEM FORMULATION

We consider the problem of estimating the unknown three-dimensional location of a target, denoted by $\mathbf{t} \in \mathbb{R}^3$, which is assumed to lie within a bounded region of interest modeled as a box of size B . The positions of N anchors are known and represented by $\mathbf{a}_i \in \mathbb{R}^3$, $i = 1, \dots, N$. Specifically, the target and anchor coordinates are given by $\mathbf{t} = [t_x, t_y, t_z]^T$ and $\mathbf{a}_i = [a_{ix}, a_{iy}, a_{iz}]^T$, and the system geometry is illustrated in Fig. 1. For each anchor-target pair, d_i , ϕ_i , and α_i denote the true distance, azimuth angle, and elevation angle, respectively.

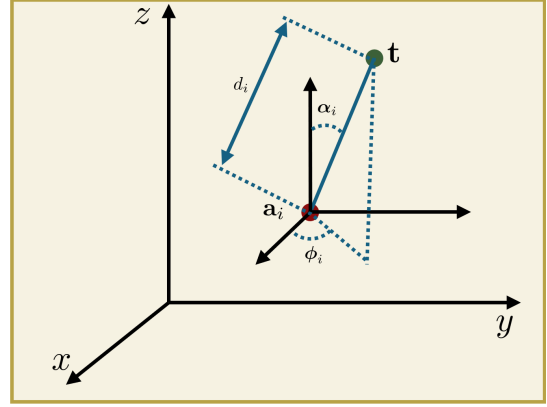


Fig. 1. 3d system model

The distance d_i , which can be estimated from the RSS at the i -th anchor is modeled as

$$P_i = P_0 - 10 \gamma \log_{10} \frac{d_i}{d_0} + n_i, \quad (1)$$

where P_0 is the reference power at distance d_0 (usually $d_0 = 1$), γ is the path-loss exponent, and $n_i \sim \mathcal{N}(0, \sigma_{n_i}^2)$ represents the log-normal shadowing noise in the logarithmic domain.

The AoA measurements are obtained using a directional antenna array and are modeled as

$$\phi_i = \arctan \left(\frac{t_y - a_{iy}}{t_x - a_{ix}} \right) + m_i, \quad (2)$$

$$\alpha_i = \arccos \left(\frac{t_z - a_{iz}}{\|\mathbf{t} - \mathbf{a}_i\|} \right) + \nu_i, \quad (3)$$

where $m_i \sim \mathcal{N}(0, \sigma_{m_i}^2)$ and $\nu_i \sim \mathcal{N}(0, \sigma_{\nu_i}^2)$ denote azimuth and elevation measurement errors, respectively.

To estimate the target position, one can form the conditional probability density function (PDF) of the measurements given \mathbf{t} . Let the observation vector be $\boldsymbol{\theta} = [\mathbf{p}^T, \boldsymbol{\phi}^T, \boldsymbol{\alpha}^T]^T \in \mathbb{R}^{3N}$, where $\mathbf{p} = [P_1, \dots, P_N]^T$, $\boldsymbol{\phi} = [\phi_1, \dots, \phi_N]^T$, and $\boldsymbol{\alpha} = [\alpha_1, \dots, \alpha_N]^T$. Assuming independent Gaussian measurement noise, the likelihood function can be written as

$$P(\boldsymbol{\theta} | \mathbf{t}) = \prod_{j=1}^3 \prod_{i=1}^N \frac{1}{\sqrt{2\pi\sigma_{i+(j-1)N}^2}} \times \exp \left\{ -\frac{(\theta_{i+(j-1)N} - f_{i+(j-1)N}(\mathbf{t}))^2}{2\sigma_{i+(j-1)N}^2} \right\}, \quad (4)$$

where

$$\mathbf{f}(\mathbf{t}) = [f_1(\mathbf{t}), \dots, f_{3N}(\mathbf{t})] \quad (5)$$

$$= [P_0 - 10\gamma \log_{10} \left(\frac{d_1}{d_0} \right), \dots, P_0 - 10\gamma \log_{10} \left(\frac{d_N}{d_0} \right),]$$

$$\arctan \left(\frac{t_y - a_{1y}}{t_x - a_{1x}} \right), \dots, \arctan \left(\frac{t_y - a_{Ny}}{t_x - a_{Nx}} \right),$$

$$\arccos \left(\frac{t_z - a_{1z}}{\|\mathbf{t} - \mathbf{a}_1\|} \right), \dots, \arccos \left(\frac{t_z - a_{Nz}}{\|\mathbf{t} - \mathbf{a}_N\|} \right)]$$

(6)

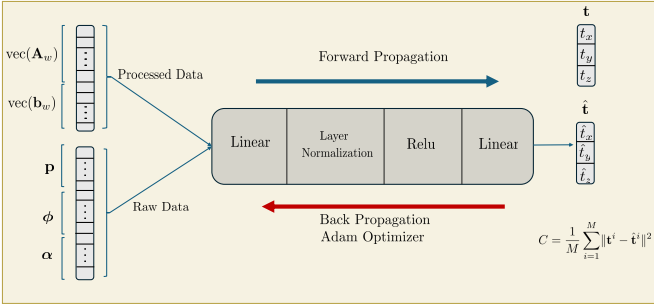


Fig. 2. Illustration of the MLP-based positioning network. The model can operate on two types of inputs: preprocessed features derived from the WLS formulation ($\text{vec}(\mathbf{A}_w)$, $\text{vec}(\mathbf{b}_w)$) or raw measurements (\mathbf{p} , ϕ , α). The network consists of a linear layer, layer normalization, ReLU activation, and a final linear layer to predict the 3D target position $\hat{\mathbf{t}} = [\hat{t}_x, \hat{t}_y, \hat{t}_z]^T$. Training is performed using the MSE loss with the Adam optimizer.

Directly maximizing this likelihood is challenging due to the nonconvexity of the resulting optimization problem.

An alternative, suboptimal approach is the WLS solution proposed in [3], which approximates the nonlinear model as a linear system:

$$\min_{\mathbf{t}} \|\mathbf{W}(\mathbf{A}\mathbf{t} - \mathbf{b})\|, \quad (7)$$

with closed-form solution

$$\hat{\mathbf{t}} = (\mathbf{A}^T \mathbf{W}^T \mathbf{W} \mathbf{A})^{-1} (\mathbf{A}^T \mathbf{W}^T \mathbf{W} \mathbf{b}), \quad (8)$$

where the matrices have dimensions $\mathbf{A} \in \mathbb{R}^{3N \times 3}$, $\mathbf{b} \in \mathbb{R}^{3N \times 1}$, and $\mathbf{W} \in \mathbb{R}^{3N \times 3N}$, with detailed definitions provided in the Appendix.

Although WLS provides a computationally efficient estimator, it suffers from several limitations in practical positioning systems. Its performance relies on assumptions such as accurate linearization, Gaussian and independent noise, and correctly specified weighting, which are only approximately satisfied in practice. In particular, linearization assumes small measurement noise for all observations, but performance is much more sensitive to AoA noise than RSS noise. Small angular errors in AoA measurements can lead to large position errors due to the geometric relationship between angles and location [10]. Moreover, linearized formulations of hybrid RSS/AoA models do not produce strictly independent Gaussian errors, since the linearization propagates measurement noise nonlinearly [7].

The measurement noise is also heterogeneous across anchors, meaning that different anchors may have different variances [7]. The weighting matrix proposed in [3], while reasonable, is not guaranteed to be optimal; if it is uniform or estimated incorrectly, the WLS solution can be biased. These factors collectively limit the accuracy of WLS, particularly in scenarios with high AoA noise.

To address these limitations, we propose using MLP to learn a robust mapping from the WLS input parameters to the target position. Our approach can implicitly account for nonlinearities, heterogeneous noise, and suboptimal weighting,

leading to nearly constant performance across different SNR levels, unlike conventional WLS.

III. DEEP LEARNING BASED POSITIONING

To address the limitations of WLS, including nonlinear noise propagation, heterogeneous measurement variances, and sensitivity to weighting accuracy, we consider two MLP-based positioning approaches within the same MLP architecture. The first approach leverages the model-based preprocessing proposed in [3], while the second directly operates on raw measurements. This allows us to isolate and evaluate the impact of preprocessing on learning performance, while maintaining an identical network structure and training procedure. Figure 2 shows the MLP network architecture for the cases of raw and preprocessed inputs.

A. Learning with preprocessed measurements

In the first approach, the MLP is trained using the linearized system parameters derived from the WLS formulation. Specifically, the matrices \mathbf{A} , \mathbf{b} , and the weighting matrix \mathbf{W} are used as input features, while the true target position \mathbf{t} serves as the label.

Each training sample is formed by preprocessing the inputs into a single feature vector

$$\mathbf{x}^i = [\text{vec}(\mathbf{A}_w)^T, \text{vec}(\mathbf{b}_w)^T]^T \in \mathbb{R}^{12N \times 1}, \quad (9)$$

where $\mathbf{A}_w = \mathbf{W}\mathbf{A} \in \mathbb{R}^{3N \times 3}$ and $\mathbf{b}_w = \mathbf{W}\mathbf{b} \in \mathbb{R}^{3N \times 1}$.

The training dataset is constructed as

$$\mathbf{X} = [\mathbf{x}^1, \dots, \mathbf{x}^M] \in \mathbb{R}^{12N \times M}, \quad \mathbf{Y} = [\mathbf{t}^1, \dots, \mathbf{t}^M] \in \mathbb{R}^{3 \times M},$$

where M denotes the number of training samples and \mathbf{t}^i is the target position corresponding to \mathbf{x}^i .

The MLP is trained to minimize the mean squared error (MSE)

$$C = \frac{1}{M} \sum_{i=1}^M \|\mathbf{t}^i - \hat{\mathbf{t}}^i\|^2, \quad (10)$$

using Adam optimizer.

B. Learning with raw measurements

To evaluate the role of model-based preprocessing, we also train an MLP using the raw measurement vector as input. In this case, the input matrix is defined as

$$\mathbf{X}_{\text{raw}} = [\boldsymbol{\theta}^1, \dots, \boldsymbol{\theta}^M] \in \mathbb{R}^{3N \times M},$$

where $\boldsymbol{\theta}^i = [\mathbf{p}^{iT}, \phi^{iT}, \alpha^{iT}]^T$ contains the raw RSS and AoA measurements for the i -th sample. The output labels are identical to those used in the preprocessed case, i.e., $\mathbf{Y} = [\mathbf{t}^1, \dots, \mathbf{t}^M]$.

Apart from the input representation, only the input dimensionality differs between the two approaches, while the network architecture, training procedure, and loss function remain identical. This setup enables a fair comparison between learning from raw measurements and learning from model-informed features derived from the WLS formulation.

IV. SIMULATION RESULTS

Simulations are performed for a target constrained within a three-dimensional box of size $B = 15$, with $N = 4$ anchors. The path-loss exponent γ is assumed to vary between 2.2 and 2.8, while the receiver uses a fixed value of $\gamma = 2.5$. Other system parameters are $P_0 = -10$ dBm and $d_0 = 1$ m. The WLS and LS solutions are evaluated over 10,000 Monte Carlo iterations for each noise scenario. For the MLP-based estimators, the dataset contains 100,000 samples, of which 75% are used for training, 15% for validation, and 10% for testing. The network is trained for 300 epochs using a learning rate of 0.01. The network is trained on all SNR levels and scenarios, while testing is performed on specific noise levels to generate the performance curves. The network architecture and training setup are summarized¹ in Table I. The MLP architecture was selected through an empirical design process. An initially overparameterized network was considered to ensure sufficient modeling capacity, after which the number of layers and neurons was progressively reduced to improve generalization. Batch normalization was found ineffective in this setting and was therefore not adopted, while layer normalization was employed to stabilize training under varying noise conditions. The final architecture provides a favorable trade-off between estimation accuracy and model complexity.

To evaluate performance, the RMSE of the estimated target positions is computed as

$$\text{RMSE} = \sqrt{\frac{1}{M_c} \sum_{i=1}^{M_c} \|\mathbf{t}_i - \hat{\mathbf{t}}_i\|^2}, \quad (11)$$

where M_c denotes the number of Monte Carlo iterations, \mathbf{t}_i is the true target position, and $\hat{\mathbf{t}}_i$ is the corresponding estimate. For the MLP-based estimators, the input features are normalized to have zero mean and unit variance, ensuring that all features have comparable statistical scales. This preprocessing step facilitates stable and efficient network training across different types of measurements. The methods considered as the benchmark in this study are named as follows: the baseline methods from [3], [4], and [5] are referred to as WLS, LS, and SR-WLS, respectively, while the proposed deep learning-based approach is referred to as "MLP-Processed Data" and "MLP-Raw Data".

Figure 3 shows the RMSE as a function of the RSS noise standard deviation σ_n . It can be observed that the MLP-based estimator trained with preprocessed measurements using the linearization method in [3] consistently outperforms all other methods, including WLS, SR-WLS, and LS. In contrast, training the same network on raw measurements does not provide any significant improvement over the conventional estimators.

Figures 4 and 5 depict the RMSE versus azimuth and elevation noise, σ_m and σ_ν , respectively. The results for both angular measurements are similar: MLP-preprocessed data

TABLE I
DNN ARCHITECTURE AND PARAMETERS

Layer	Type	Output Size	Notes / Parameters
1	Linear	128	Input: \mathbf{x}^i / θ^i
2	LayerNorm	128	Normalizes features across layer
3	ReLU	128	Activation function
4	Linear	3	Output: $\hat{\mathbf{t}}_i$

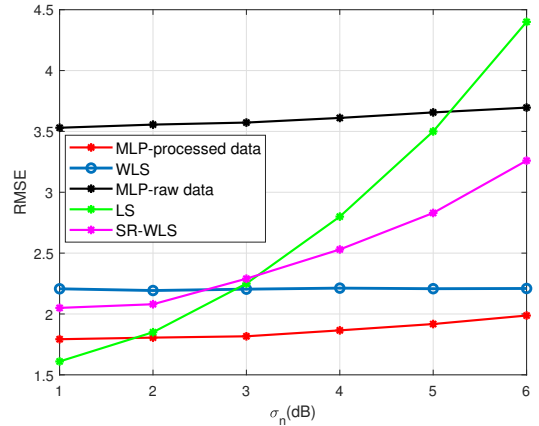


Fig. 3. RMSE of the target position versus RSS noise standard deviation σ_{n_i} .

achieves better performance than SR-WLS and LS, while its performance is comparable to WLS. Furthermore, the advantage of using preprocessed measurements persists across all noise levels, demonstrating that the proposed approach provides robust performance under a wide range of noise conditions.

V. CONCLUSION

In this paper, we proposed a MLP-based approach for hybrid RSS/AoA positioning, capturing nonlinearities that limit conventional linear estimators. We showed that preprocessing measurements using a linearization method significantly improves the performance of the MLP network compared to raw data. Simulation results demonstrated that the proposed method consistently outperforms existing WLS, SR-WLS, and LS approaches under RSS and angular noise. These findings highlight that deep learning with geometry-aware preprocessing enables robust and accurate positioning across a wide range of noise conditions.

REFERENCES

- [1] L. Italiano, B. Camajori Tedeschini, M. Brambilla, H. Huang, M. Nicoli, and H. Wymeersch, "A tutorial on 5g positioning," *IEEE Communications Surveys & Tutorials*, vol. 27, no. 3, pp. 1488–1535, 2025.
- [2] Y. Yang, M. Chen, Y. Blankenship, J. Lee, Z. Ghassemlooy, J. Cheng, and S. Mao, "Positioning using wireless networks: Applications, recent progress, and future challenges," *IEEE Journal on Selected Areas in Communications*, vol. 42, no. 9, pp. 2149–2178, 2024.
- [3] S. Tomic, M. Beko, R. Dinis, and P. Montezuma, "A closed-form solution for rss/aoa target localization by spherical coordinates conversion," *IEEE Wireless Communications Letters*, vol. 5, no. 6, pp. 680–683, 2016.

¹The dataset and trained networks are available at <https://your-link-here>.

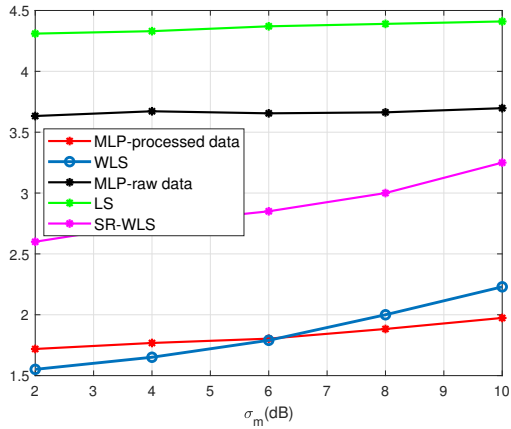


Fig. 4. RMSE of the target position versus azimuth noise standard deviation σ_{m_i} .

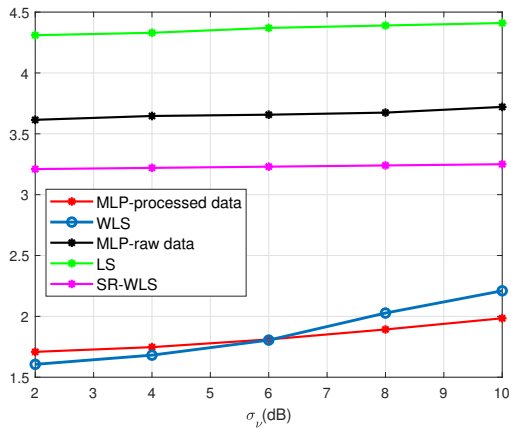


Fig. 5. RMSE of the target position versus elevation noise standard deviation σ_{n_i} .

- [4] K. Yu, “3-d localization error analysis in wireless networks,” *IEEE Transactions on Wireless Communications*, vol. 6, no. 10, pp. 3472–3481, 2007.
- [5] S. Tomic, M. Beko, and M. Tuba, “A linear estimator for network localization using integrated rss and aoa measurements,” *IEEE Signal Processing Letters*, vol. 26, no. 3, pp. 405–409, 2019.
- [6] Y. Yang, H. Yang, and F. Meng, “A bluetooth indoor positioning system based on deep learning with rss and aoa,” *Sensors*, vol. 25, no. 9, p. 2834, 2025.
- [7] S. Kang, T. Kim, and W. Chung, “Hybrid rss/aoa localization using approximated weighted least square in wireless sensor networks,” *Sensors*, vol. 20, no. 4, p. 1159, 2020.
- [8] Anonymous, “Mathematical foundations of deep learning,” *Preprints.org*, 2025, demonstrates neural networks’ universal nonlinear approximation capability. [Online]. Available: <https://www.preprints.org/manuscript/202502.0272/v6>
- [9] D. Burghal, A. T. Ravi, V. Rao, A. A. Alghafis, and A. F. Molisch, “A comprehensive survey of machine learning based localization with wireless signals,” *arXiv preprint arXiv:2012.11171*, 2020.
- [10] M. H. AlSharif, M. Ba’adani, F. Toro, K. Ghamdi, S. Zahraei, M. Abdulmohsin, and A. Al-Jarro, “In-pipe localization for pipeline intervention gadgets,” in *Abu Dhabi International Petroleum Exhibition and Conference*. SPE, 2023, p. D031S117R001.

APPENDIX

Assuming the noise is negligible, (1), (2), and (3) can be approximated as

$$\lambda_i \|\mathbf{t} - \mathbf{a}_i\| \approx \eta d_0, \quad i = 1, \dots, N \quad (12)$$

$$\mathbf{c}_i^T (\mathbf{t} - \mathbf{a}_i) \approx 0, \quad i = 1, \dots, N \quad (13)$$

$$\mathbf{k}^T (\mathbf{t} - \mathbf{a}_i) \approx \|\mathbf{x} - \mathbf{a}\| \cos(\alpha_i), \quad i = 1, \dots, N \quad (14)$$

where $\lambda_i = 10^{P_i/10\gamma}$, $\eta = 10^{P_0/10\gamma}$, $\mathbf{c}_i = [-\sin(\phi_i), \cos(\phi_i), 0]^T$, $\mathbf{k} = [0, 0, 1]^T$.

If each $\mathbf{t} - \mathbf{a}_i$ in the spherical domain is represented as

$$\mathbf{t} - \mathbf{a}_i = r_i \mathbf{u}_i, \quad (15)$$

where $r_i > 0$ is the distance from the origin and $\|\mathbf{u}_i\| = 1$ is the directional unit vector obtained from the AoA as

$$\mathbf{u}_i = [\cos(\phi_i) \sin(\alpha_i), \sin(\phi_i) \sin(\alpha_i), \cos(\alpha_i)]^T, \quad (16)$$

then, multiplying (12), (13), and (14) by $\mathbf{u}_i^T \mathbf{u}_i$ gives

$$\lambda_i \mathbf{u}_i^T r_i \mathbf{u}_i \approx \eta d_0 \Leftrightarrow \lambda_i \mathbf{u}_i^T (\mathbf{t} - \mathbf{a}_i) \approx \eta d_0, \quad (17)$$

$$\mathbf{k}^T r_i \mathbf{u}_i \approx \mathbf{u}_i^T r_i \mathbf{u}_i \cos(\alpha_i) \Leftrightarrow (\cos(\alpha_i) \mathbf{u}_i - \mathbf{k})^T (\mathbf{t} - \mathbf{a}_i) \approx 0, \quad (18)$$

From (13), (17), and (18), the matrices \mathbf{A} and \mathbf{b} can be directly constructed as

$$\mathbf{A} = \begin{bmatrix} \vdots & & \\ \lambda_i \mathbf{u}_i^T & & \\ \vdots & & \\ \mathbf{c}_i^T & & \\ \vdots & & \\ (\cos(\alpha_i) \mathbf{u}_i - \mathbf{k})^T & & \\ \vdots & & \end{bmatrix}, \quad \mathbf{b} = \begin{bmatrix} \vdots & & \\ \lambda_i \mathbf{u}_i^T \mathbf{a}_i + \eta d_0 & & \\ \vdots & & \\ \mathbf{c}_i^T \mathbf{a}_i & & \\ \vdots & & \\ (\cos(\alpha_i) \mathbf{u}_i - \mathbf{k})^T \mathbf{a}_i & & \\ \vdots & & \end{bmatrix}. \quad (19)$$

The weighting matrix is constructed as $\mathbf{W} = \mathbf{I}_3 \otimes \mathbf{w}$, where \mathbf{I}_3 denotes the 3×3 identity matrix and $\mathbf{w} \in \mathbb{R}^{N \times 1}$ contains the weighting coefficients $w_i = 1 - \frac{\hat{d}_i}{\sum_{j=1}^N \hat{d}_j}$, with $\hat{d}_i = d_0 10^{\frac{P_0 - P_i}{10\gamma}}$. The symbol \otimes denotes Kronecker product.